

Imaging Organic and Biological Materials with Low Voltage Scanning Electron Microscopy

Application Note

Hamdallah A. Béarat, Ph.D.

Introduction

Scanning electron microscopy has become a popular imaging tool in different areas of science and engineering^[1-7]. Being able to elucidate the structure of a material at the micro-and/or the nano-scale level is indeed crucial to characterizing the material, understanding its mechanism and mode of formation, and explaining/predicting its properties and performance under a given set of environmental or load conditions^[1,2,3,8,9]. Secondary electron imaging is commonly used to reveal surface topography, grain morphology and size, phase composition, and fracture profile. In such cases highest resolution and contrast are needed to illustrate the finest structural features. However, imaging of organic and biological specimens represents a real challenges to investigators. We discussed briefly in a previous note^[10] the options available to overcome these difficulties. With the Agilent 8500 low voltage scanning electron microscope (FE-SEM), imaging of organic and biological materials is strongly facilitated^[11,12]. For this application note, we present here imaging data obtained with Agilent 8500 FE-SEM for different

materials: (1) chemical and physical-chemical gelling of bioinjectable copolymers NC-NCA being explored as an alternative treatment for brain aneurism; (2) HeLa cervical cancer cells used to study the effect of irreversible electroporation on adherent cells; (3) biotically-precipitated calcium carbonate induced by CO₂-producing bacteria and enzyme for soil improvement.

Methodology

Data presented in this note concern samples from different areas of engineering. This includes: bioinjectable copolymers for medical application; culture cancer cells; biotic (both enzymatic- and bacterial-induced) precipitation of calcium carbonate for soil consolidation. Samples were processed and prepared in different ways, but preparation for FE-SEM imaging was minimal. Specimens are simply cut or fractured from original samples and adhered via carbon tape to aluminum stubs and loaded onto microscope stage. In the case of the HeLa cervical cancer cells, the entire electrodes plate (1 sq. in.) was adhered to the aluminum stub via C-tape and



Agilent Technologies

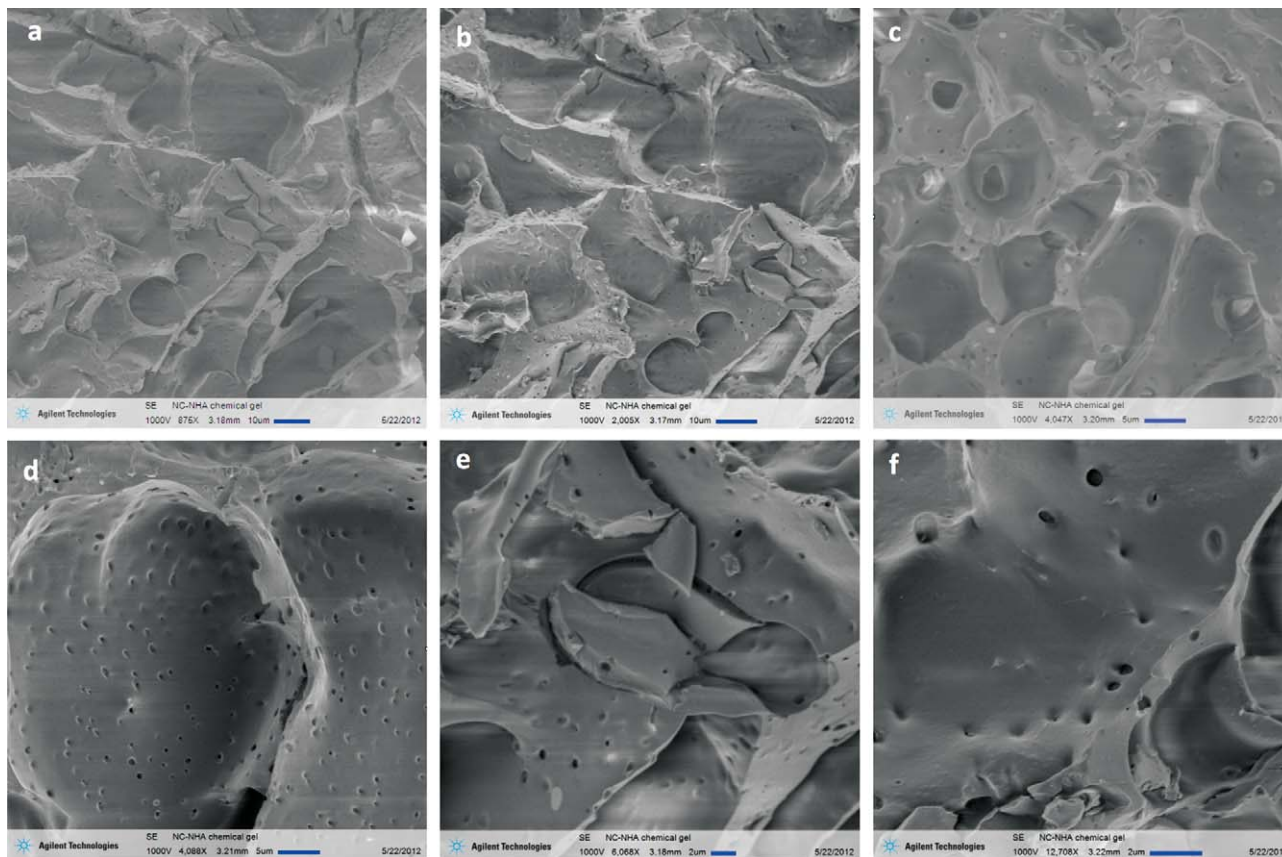


Figure 1. SE Image sequence (a through f) obtained with Agilent 8500 for NC-NCA chemical gel. Images (a–c) clearly show the gel product is porous, but homogeneous, with large pores and channels several microns across. Images (d–f) show the gel has plenty of the nano-pores (<200 nm).

mounted onto the microscope stage. The samples examined here come from the following experiments:

(1) Copolymers: Chemical gel as well as physical-chemical gel systems were investigated. The experimental procedure is described with detail in reference^[8]. The copolymers investigated here are poly(NIPAAm-co-cysteamine), abbreviated NC and poly(NIPAAm-co-HEMA-acrylate), abbreviated NCA. For SEM imaging, samples were cut with a razor blade and mounted directly onto carbon tape adhered to an aluminum stub. Physical-chemical gel material imaged here with FE-SEM is compared to material from a similar experiment

observed with E-SEM after coating with gold. Chemical gel material is imaged first here. No previous images are available for comparison.

(2) Cervical cancer cells: These are the famous HeLa cells. The cells were grown on a microelectrode array and tested with variable voltage pulses. The aim of the experiment was to study the effect of irreversible electroporation on adherent cells. However, there might be a failure in the chemical fixing process of the cells at the end of experiment that caused damage to the membrane of most cells.

(3) Biotically-precipitated calcium carbonate: Samples studied here come from different experiments. In the first, quartz sand was consolidated by calcium carbonate (calcite) precipitated by the action of a CO₂ producing enzyme^[9]. The sample was a fragment of a consolidated core sample that was adhered via carbon tape onto the aluminum stub. The second comes from an experiment done with CO₂-producing bacteria^[12]. Peculiarly, calcite did not precipitate in the sand core, but as a pink crust that formed somewhere else in the system. The sample studied here was a fragment broken from this pink crust that was divided into two pieces of which face and back were imaged.

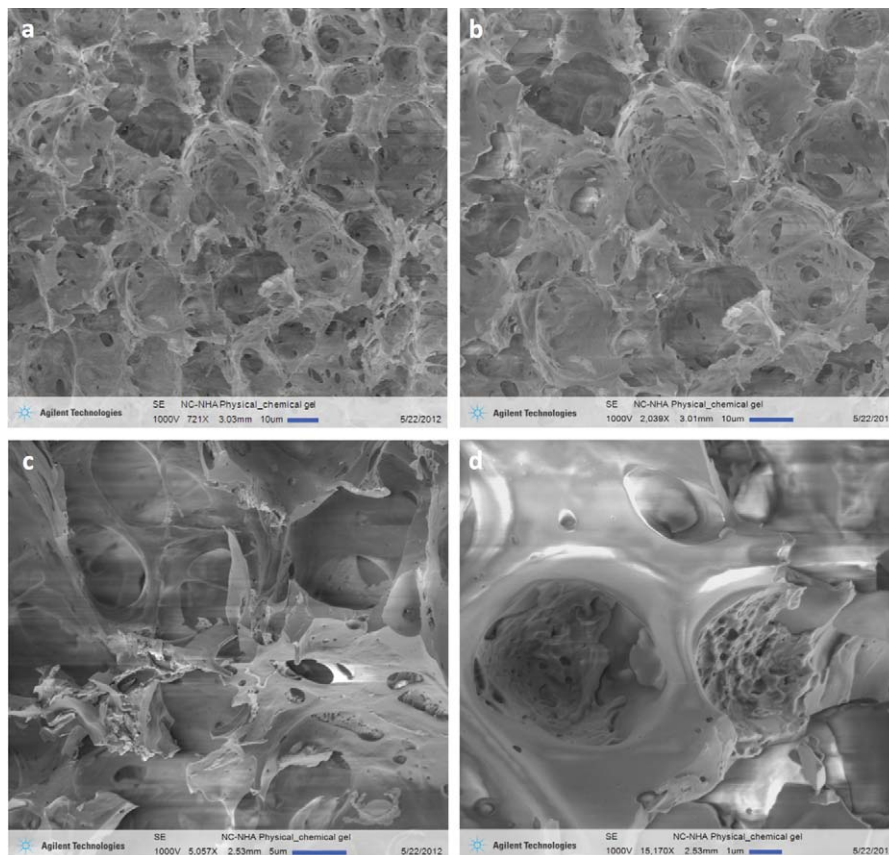


Figure 2. SE Image sequence (a through d) obtained with Agilent 8500 for NC-NCA physical-chemical gel . Images (a) and (b) clearly show that the gel product has a spongy with large pores and channels several microns across. Images (c) and (d) show the gel is heterogeneous with a porous phase forming in the cavities of the other. Image (d) also show some sporadic nano-scale pores in the matrix phase.

Results and Discussion

1. FE-SEM Imaging of copolymer chemical and physical-chemical gelling systems:

The gelling systems investigated here as possible treatment for cerebral aneurism are made of the copolymers poly(NIPAAm-co-cysteamine) and poly(NIPAAm-co-HEMA-acrylate). These hydrogels undergo gelation through dual mechanisms: temperature sensitivity (physical gelation) and chemical crosslinking (chemical gelation). Full description of the preparation and characterization of these gels are given in details^[8]. The aim of imaging is to envision the evolution of micro- and nano-structure of chemical gel and compare with

that of the physical-chemical gel. Figure 1 shows SE image sequence obtained with Agilent 8500 for NC-NCA chemical gel. Images clearly show the gel product is porous and homogeneous, with large pores and channels several microns across. At higher magnification, the gel is shown to have plenty of nano-pores (<200 nm). In contrast, the physical-chemical gel, while still having a spongy structure with micro pores and channels, has a heterogeneous composition. A minor grainy porous phase has formed in the cavities of the major (matrix) phase. The latter has only sporadic nano-pores. These observations suggest that structural (phase) changes during chemical

gelation are different from those occurring during physical-chemical gelation. In the former, gelation occurs through chemical reaction (cross-linking) of the copolymers at constant temperature which is below their LCST (lower critical solution temperature). Whereas in the physical-chemical gelation, the temperature rises and allows physical and chemical gelation processes to occur simultaneously. This means some of physical gel gets trapped in the cavities of the chemical gel without having the chance for the copolymers to cross-link completely. This is in complete accord with X-ray diffraction and SAXS studies.

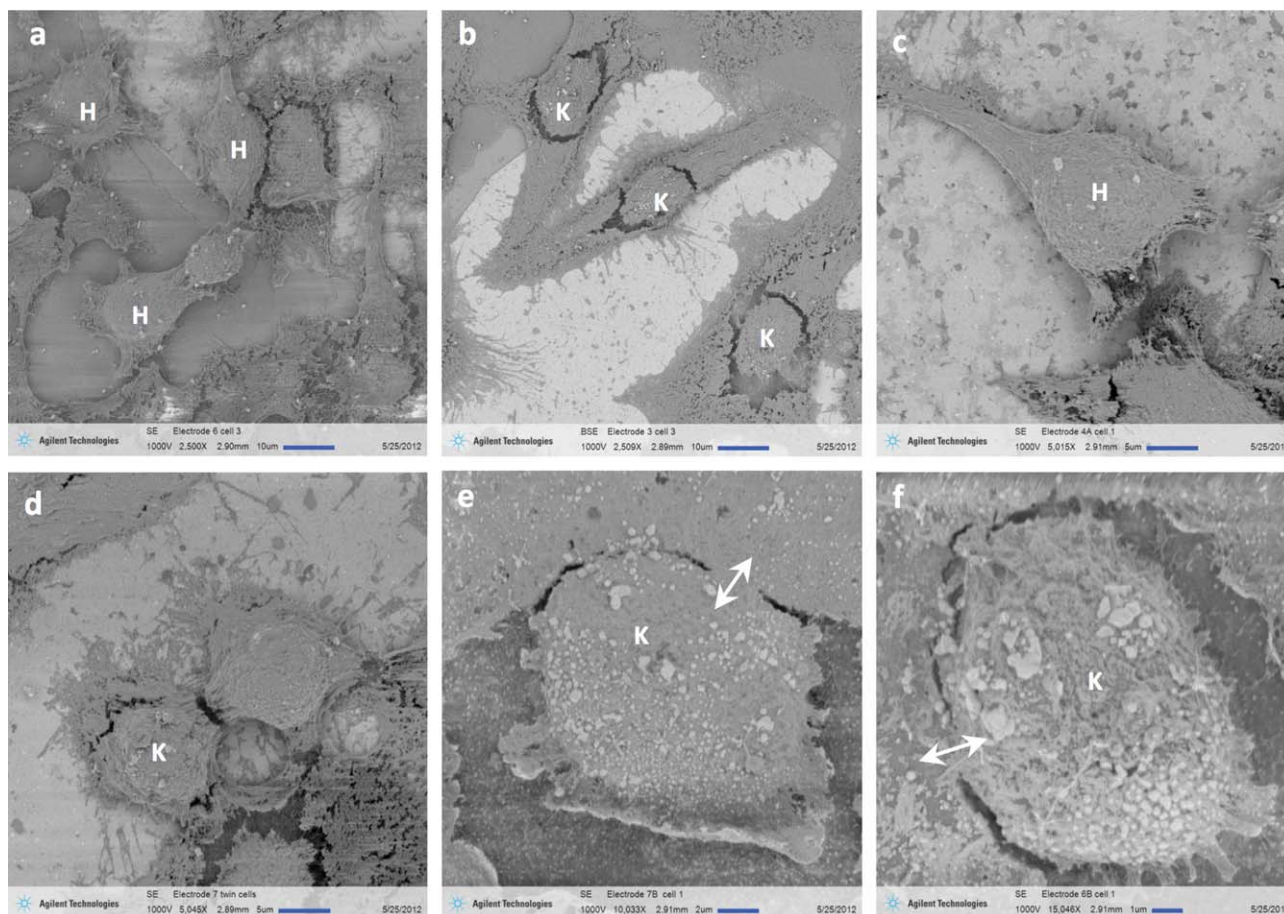


Figure 3. SE Images (a through f) obtained with Agilent 8500 for HeLa cervical cancer cells from an electroporation experiment. Cells indicated by H are considered healthy cells after the fixing process is finished. Whereas those indicated by K are cells killed by the fixing process or by the application of the electric pulse. In the latter case, cell membrane is being broken and nucleus separates from the rest of cell; some remnant connection may still be seen, as indicated by the double arrows.

2. FE-SEM Imaging of HeLa cervical cancer cells:

These are cultured cells tested with variable electrical pulse. The whole electrode array with the tested and “fixed” cells was observed. The chemical fixing process might have been incomplete and caused destruction of the cells on most electrodes (control, 4V, 8V, and 12V). However, our main goal was to demonstrate that Agilent 8500 LV-SEM can be used efficiently to image biological materials, including cancer cells. Successful imaging, indeed, help bioengineers and microbiologists optimizing the experimental procedure. These

both goals were served by the data acquired. Figure 3 shows SE images taken with Agilent 8500 FE-SEM of the aforementioned HeLa cervical cancer cells. The images show some of the cells were healthy at the end of the pulse experiments and survived the fixing process. These are indicated by the letter H on the images. Other cells, even sitting on the control electrode or on the substrate away from any electrode, have been killed. They are indicated by the letter K on the images. In the latter, the cell membrane has ruptured and the nucleus separated from the rest of the cell. The experiment shall be optimized and further imaging

is needed to elucidate how the cell membrane interacts with an increasing electric pulse and whether nano-pores will open in it, thus allowing gene delivery into the cancer cells.

3. FE-SEM Imaging of calcium carbonate precipitation for soil improvement:

Data presented here relate to two experiments^[9]. In the first experiment, an enzyme extracted from plants is injected into the sandy soil. The enzyme convert urea into CO₂ and NH₃. Ammonia raises the pH and CO₂ combines with calcium ions to form calcium carbonate (mostly calcite),

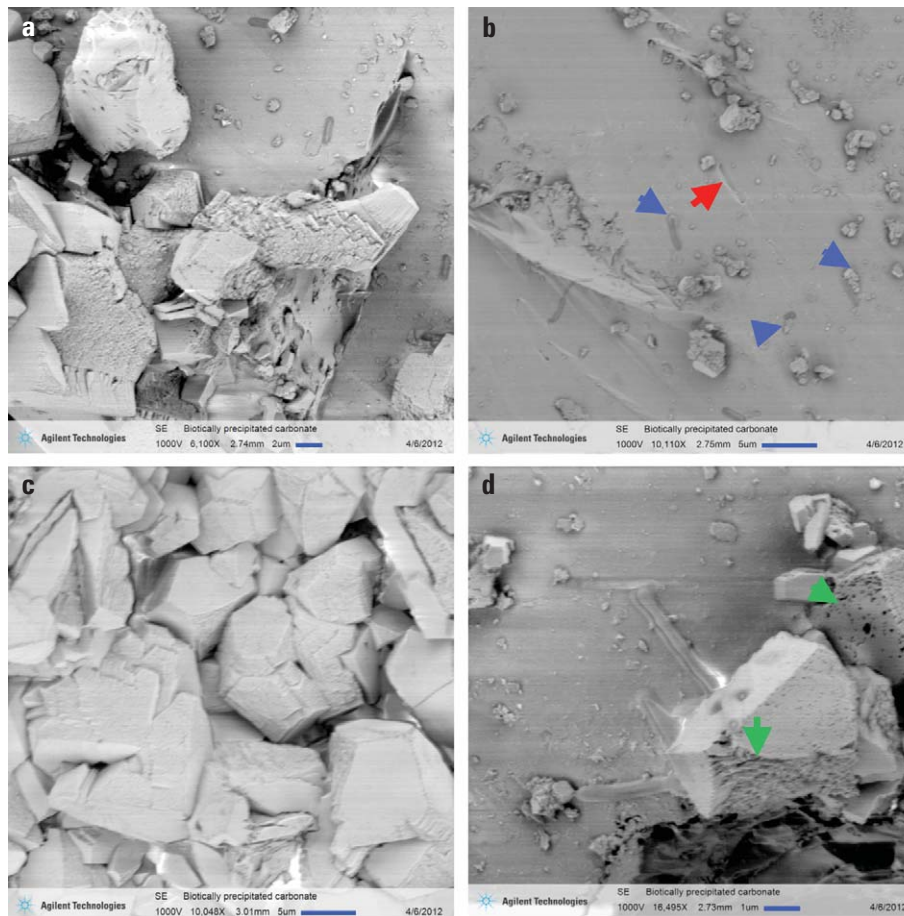


Figure 4. SE images obtained with Agilent 8500 FE-SEM for a quartz sand sediment consolidated with enzyme induced precipitation of calcium carbonate (calcite): (a) growing calcite crystals; (b) indentation of quartz surface (red arrow) and calcite nucleation (blue arrows) where enzyme molecules adhere to quartz surface; (c) well grown and cementing calcite crystals; (d) high magnification image showing growing calcite crystals to be layered and porous (green arrows).

which acts as a cement to consolidate the soil. In the second experiment, denitrifying bacteria is injected with “its food” in the soil. CO_2 is produced as a result of bacterial metabolism and combines with calcium ions to form calcium carbonate, which serves as a cement in sandy soil improvement. The first experiment worked perfectly and quartz sand was cemented by the precipitated carbonate (calcite). The other experiment, however, gave some peculiar results. Calcite did precipitate in the sand core, but somewhere else in the system. Geotechnical engineers are investigating this issue. But, as far as the FE-SEM imaging is concerned,

the sample examined met perfectly our goal of imaging bacterial cells without the need for sample coating. In both cases, high resolution images with excellent contrast were obtained for the biological and organic samples with minimal charging and no damage to them.

Figure 4 shows images of enzymatically-induced calcium carbonate precipitation. Full comment on these images is given in a previous application note^[10]. FE-SEM imaging has permitted to better understand the mechanism of the reaction process and the different aspect of the role played by the enzyme^[10].

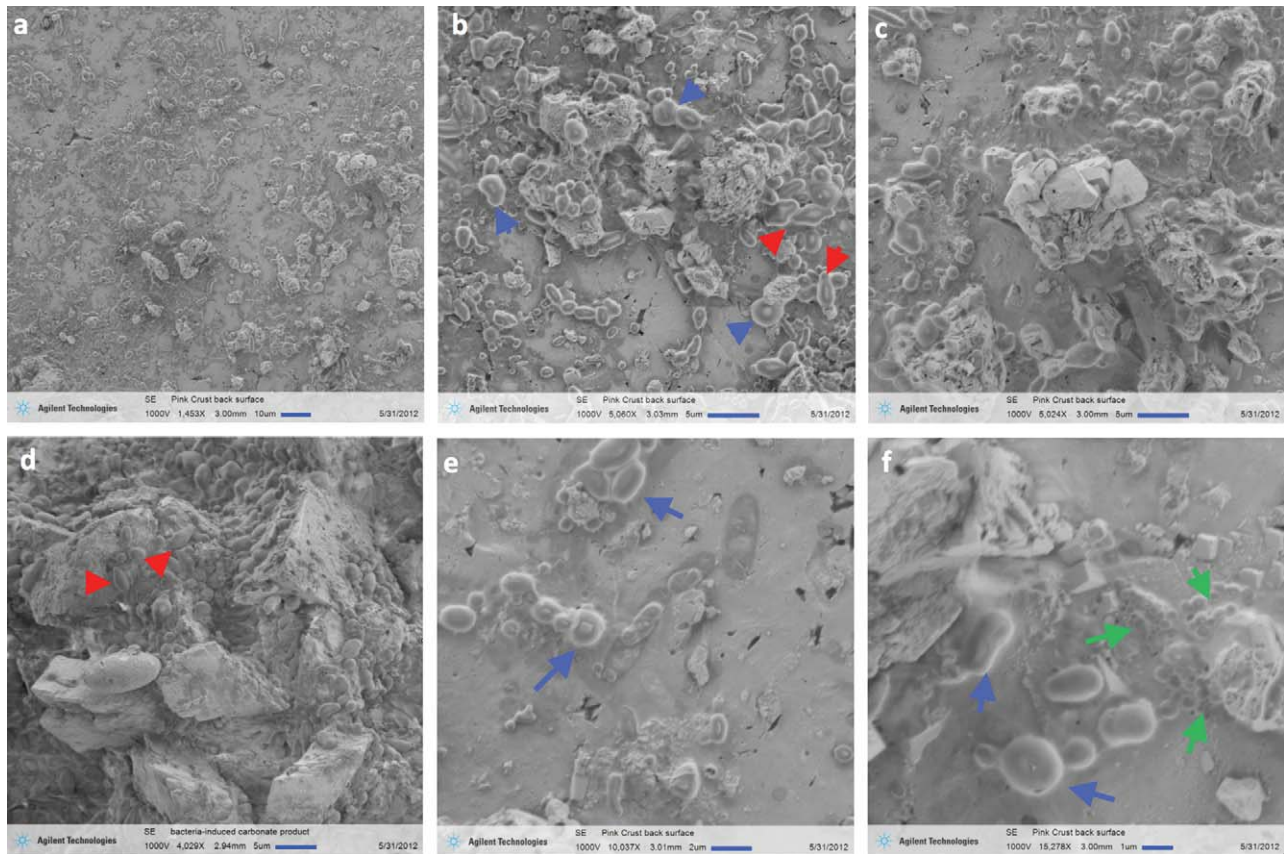


Figure 5. SE images (a–f) obtained with Agilent 8500 FE-SEM for bacteria-induced carbonate precipitation. Note the intergrowth of calcite crystals and bacterial cells. In many locations, bacterial cells or their remnant skeletons are buried inside the carbonate crystals. Note also the bimodal size of bacteria: normal (0.5–5 μm, blue arrows) and nanobacteria (100–300 nm, green arrows). Some bacterial cells are spherical, some ellipsoidal, and some rod-shaped; some cells are actually in dividing stage or spore stage (red arrows).

In Figure 5 a set of SE images obtained with the Agilent 8500 FE-SEM is presented for the experiment with denitrifying bacteria. These images reveal many features of the biotic process. Bacterial cells are very abundant in the carbonate product. Some bacterial cells are spherical, some ellipsoidal, and some others rod-shaped. Some bacterial cells are actually in dividing stage and others in spore stage. It is worth noting the normal bimodal size of bacteria cells is 0.5–5 μm with most being 1 μm and nanobacteria size being 100–300 nm. This is consistent with observation of fossilized bacteria in hydrothermal travertine (a rock composed of calcium carbonate, too)^[2]. Note also the intergrowth of

calcite crystals and bacterial cells. In many locations, bacterial cells or their remnant skeletons are buried inside the carbonate crystals. The latter have therefore a spongy porous internal structure. It was also observed that the outside surface of this carbonate product crust is well sealed, with carbonate crystals intermixed with bacterial bodies and crystal edges well rounded. Full interpretation of the entire body of data acquired for both carbonate precipitation experiments and explanation of the different implication to geotechnical engineering, biomineralization, and sedimentology shall be published soon in a peer-reviewed journal.

Conclusions

Using Agilent 8500 FE-SEM, it was quite possible to image, with high resolution and excellent contrast, insulating materials such as organic (copolymers and enzyme) and biological (cancer cells and bacteria), without the need for a metal coating or radiation damage to the samples. These analyses are otherwise not as feasible using other FE-SEMs: cold field emission SEM operating at low voltage and E-SEM, respectively. It is fair to say also that Agilent 8500 FE-SEM is more helpful in studying sensitive organic or biological samples such as enzymes, cell membranes, neurons, bacteria, biofilms, and biogels, when compared to other FE-SEMs currently available.

References

- [1] De Winter, D.A.M., Schneijdenberg, C.T.W.M., Lebbink, M.N., Lich, B., Verkleij, A.J., Drury, M.R., and Humbel, B.M., Tomography of insulating biological and geological materials using focused ion beam (FIB) sectioning and low-kV BSE imaging. *Journal of Microscopy*, **233** [3] 2009, 372–383.
- [2] Folk, R.L., SEM imaging of bacteria and nanobacteria in carbonate sediments and rocks. *Journal of Sedimentary Petrology*, **63** [5] 1993, 990–999.
- [3] Béarat, H., McKelvy, M.J., Chizmeshya, A.V.G., Gormley, D., Nunez, R., Carpenter, R.W., Squires, K., and Wolf, G., 2006, Carbon Sequestration via Aqueous Olivine Mineral Carbonation: Role of Passivating Layer Formation. *Environ. Sci. Technol.* **40**, 4802–4808.
- [4] Donald, A.M., The use of environmental scanning electron microscopy for imaging wet and insulating materials. *Nature Materials*, **2**, August 2003, 511–516.
- [5] Moran, P., and Coats, B., Biological Sample Preparation for SEM Imaging of Porcine Retina. *Microscopy Today*, **20** [2] 2012, 28–31.
- [6] Muscariello, L., Rosso, F., Marino, G., Giordano, A., Barbarisi, M., Cafiero, G., and Barbarisi, A., A critical overview of ESEM applications in the biological field. *Journal of Cellular Physiology*, **205** [3] 2005, 328–334.
- [7] Drobne, D., Milani, M., Lešer, V., and Tatti, F., Surface damage induced by FIB milling and imaging of biological samples is controllable. *Microsc. Res. Tech.* **70** (2007) 895–903.
- [8] Bearat, H.H., Lee, B.H., and Vernon, B.L., Comparison of properties between NIPAAm-based simultaneously physically and chemically gelling polymer systems for use *in vivo*. *Biomacromolecules* (in press).
- [9] Béarat, H.A., Hamdan, N., and Kavazanjian, E., Low voltage scanning electron microscopy imaging of biotically-precipitated calcium carbonate in soil consolidation. Paper to be submitted to *Journal of Microscopy*.
- [10] Béarat, H.A., *Low Voltage Scanning Electron Microscopy: Promises and Challenges*. Application Note #5991-0736EN, Agilent Technologies Inc. 2012, 4p.
- [11] Agilent Technologies Inc. *Low Voltage FE-SEM Examination of Organic Polymers*, Application Note # 5990-8931EN.
- [12] Agilent Technologies Inc. *Use Low Voltage FE-SEM to Overcome Challenges of Imaging Biological Specimens*. Application Note # 5990-9013EN.

Nanomeasurement Systems from Agilent Technologies

Agilent Technologies, the premier measurement company, offers high-precision, modular nanomeasurement solutions for research, industry, and education. Exceptional worldwide support is provided by experienced application scientists and technical service personnel. Agilent's leading-edge R&D laboratories ensure the continued, timely introduction and optimization of innovative, easy-to-use nanomeasure system technologies.

www.agilent.com/find/nano

Americas

Canada	(877) 894 4414
Latin America	305 269 7500
United States	(800) 829 4444

Asia Pacific

Australia	1 800 629 485
China	800 810 0189
Hong Kong	800 938 693
India	1 800 112 929
Japan	0120 (421) 345
Korea	080 769 0800
Malaysia	1 800 888 848
Singapore	1 800 375 8100
Taiwan	0800 047 866
Thailand	1 800 226 008

Europe & Middle East

Austria	43 (0) 1 360 277 1571
Belgium	32 (0) 2 404 93 40
Denmark	45 70 13 15 15
Finland	358 (0) 10 855 2100
France	0825 010 700*
	*0.125 €/minute
Germany	49 (0) 7031 464 6333
Ireland	1890 924 204
Israel	972-3-9288-504/544
Italy	39 02 92 60 8484
Netherlands	31 (0) 20 547 2111
Spain	34 (91) 631 3300
Sweden	0200-88 22 55
Switzerland	0800 80 53 53
United Kingdom	44 (0) 118 9276201

Other European Countries:

www.agilent.com/find/contactus

Product specifications and descriptions in this document subject to change without notice.

© Agilent Technologies, Inc. 2012

Printed in USA, June 27, 2012

5991-0791EN